Formation of metal nanostructures under X-ray radiation in films of interpolyelectrolyte complexes with different silver ion content*

K. V. Mkrtchyan,[a] A. A. Zezin,[a,b]★ E. A. Zezina,[b] S. S. Abramchuk,[c] and I. A. Baranova[b]

[a]*N. S. Enikolopov Institute of Synthetic Polymeric Materials, Russian Academy of Sciences, 70 ul. Profsoyuznaya, 117393 Moscow, Russian Federation*
[b]*Department of Chemistry, Lomonosov Moscow State University, Build. 11, 1 Leninskie Gory, 119991 Moscow, Russian Federation. E-mail: aazezin@yandex.ru*
[c]*A. N. Nesmeyanov Institute of Organoelement Compounds, Russian Academy of Sciences, 28 ul. Vavilova, 119334 Moscow, Russian Federation*

The specific features of the formation of metal nanoparticles under X-ray radiation in interpolyelectrolyte complex (IPEC) films based on polyacrylic acid and polyethyleneimine with different silver ion content were studied. IPEC films were irradiated in aqueous-alcoholic medium. Electron microscopy demonstrated that the formation of silver nanoparticles occurred in zones regularly located by film thickness. It was found that nanoparticle size and spatial distribution in IPEC films depended on the initial concentration of silver ions within the sample and on the absorbed dose of radiation. The obtained film nanocomposites are promising objects for application as antibacterial and catalytic materials.

Key words: interpolyelectrolyte complexes, polyacrylic acid, polyethyleneimine, radiation-chemical reduction, silver nanoparticles, metal polymer nanocomposites.

Over the past several decades, much attention has been paid to the development of methods for obtaining metal polymer nanocomposites in polymer films and coatings.[1—5] Materials containing silver nanoparticles serve as the basis for a wide range of functional devices, have applications in medicine, optoelectronics, and nanophotonics, and are used for the development of sensors and biosensors.[5—12]

General method of synthesis of metal polymer nanocomposites is the reduction of metal ions in polymer systems.[1—4,7—15] Matrices based on polyelectrolytes are widely used as precursors for the synthesis of metal polymer hybrid materials,[1,2,5,10] because they effectively stabilize the forming nanoparticles. The possibility of tuning the binding of metal ions and the interaction of macromolecules with the nanoparticle surface suggests the use of interpolyelectrolyte complexes (IPECs) as a polymer base for the synthesis of nanocomposites.[1—5,9,13—20]

Radiation-chemical approaches provide considerable advancement both in obtaining chemically "pure" nanoparticles with a controlled size, and in studying the formation of nanoparticles at different stages.[4,5,9,11,12,19—24] Radiation-chemical approaches were widely used for the synthesis of copper, nickel, gold, silver nanoparticles, as well as bimetallic nanoparticles in films and coatings of complexes based on polyacrylic acid—polyethyleneimine (PAA—PEI).[4,5,9,13,19,20,25—27] The properties of nanocomposite materials depend on the size of nanoparticles and their spatial distribution within the polymer matrix. Electron accelerators, γ- and X-ray radiation sources made it possible to vary the nanoparticle formation modes and to obtain composites with different structures.[4,5,19,20]

Earlier studies of the formation of copper nanoparticles showed that an increase in the concentration of metal ions in IPEC matrices leads to an increase in the efficiency of the use of X-rays. Therefore, the formation of nanocomposite materials in films and coatings with a relatively high metal ion content is promising.[4,20,26—28]

Polymer films and coatings with electrocatalytic properties and bactericidal activity were obtained in IPECs based on PAA and PEI with silver nanoparticles.[1,9] However, at present there are no systematic studies of the formation of nanostructures in irradiated IPECs with different concentrations of silver ions. The goal of this work is to study the effect of silver ion content in IPECs based on PAA—PEI on the size and the spatial distribution of silver nanoparticles in polymer films which underwent X-ray irradiation.

Experimental

The following reagents were used for sample preparation: PAA (M_w = 80000) (Sigma-Aldrich), PEI (M_w = 60000) (Serva), analytical grade formic acid, analytical grade silver nitrate.

* Based on the materials of the XXI Mendeleev Congress on General and Applied Chemistry (September 9—13, 2019, St. Petersburg, Russia).

Published in Russian in *Izvestiya Akademii Nauk. Seriya Khimicheskaya,* No. 9, pp. 1731—1739, September, 2020.
1066-5285/20/6909-1731

Preparation of films of stoichiometric complexes PAA—PEI is described in detail in previously published works.[19,20,26]

Silver ions were sorbed into films of PAA—PEI complexes under low light to obtain PAA—PEI—Ag^+ complexes. Silver ions (25 mL) were sorbed for 48 h from an aqueous solution of $AgNO_3$ into polymer films with a diameter of 50 mm and a thickness of 150 μm at room temperature. The concentration of $AgNO_3$ in the solution was 1.2, 0.4, and 0.02 wt.% for films containing 6.0, 2.0, and 0.1 wt.% silver ions, respectively. The concentration of silver ions in the polymer films was determined based on the difference in the absorption of silver ions at 290 nm in aqueous solutions before and after sorption using a Lambda 9 UV visible range spectrometer (Perkin Elmer).

The obtained samples were irradiated on an X-ray unit with a 5-BKhV-6W tube (50 kV) in an aqueous-alcoholic mixture with a 10 vol.% ethanol content. The irradiated solution was bubbled with high purity grade argon throughout the entire irradiation process to prevent oxidation by oxygen dissolved in water and to create an inert environment. The source dose rate was 17 Gy s^{-1}. For polymer films containing Ag^+ ions, the dose rate was calculated taking into account the mass absorption coefficients and the effective energy of X-ray quanta.[29]

The structure of the nanocomposite material was studied using a Leo-912 AB OMEGA transmission microscope (Carl Zeiss, Germany) with a resolution of 0.3 nm. A microdiffraction pattern of gold was used as a standard for calculating the interplanar distances.

Results and Discussion

The dose rate of X-ray irradiation is determined by the composition of the substance and can be calculated using mass absorption coefficients for photons with the formula

$$P = P_0 \frac{\sum_i W_i (\mu/\rho)_i}{(\mu/\rho)_0},$$

where P is the dose rate in the sample; P_0 in the dose rate in a dosimetric solution in the same irradiation geometry; W_i is the mass fraction of element i in the sample, calculated taking into account the composition of the swollen film (X = C, O, N, Ag; the contribution of hydrogen to photoelectric absorption can be neglected); $(\mu/\rho)_i$ are mass absorption coefficients for photon energy of the corresponding elements; $(\mu/\rho)_0$ is the mass absorption coefficient for photon energy of the dosimetric solution (similar, in fact, to the absorption coefficient of water).

The mass absorption coefficients for X-ray radiation of the elements of the system in question for an energy of 20 keV were: 0.014 $cm^2\ g^{-1}$ for hydrogen, 0.224 $cm^2\ g^{-1}$ for carbon, 0.387 $cm^2\ g^{-1}$ for nitrogen, 0.617 $cm^2\ g^{-1}$ for oxygen, 16.95 $cm^2\ g^{-1}$ for silver.

The applied voltage and the anode current for the X-ray unit with a 5-BKhV-6W tube was 33 kV and 80 mA, respectively. In this case, the distribution maximum is realized for X-ray quanta with an energy of 21 kV. The penetrating power of X-ray radiation with these parameters is many times greater than the thickness of the irradiated film. To calculate the rates of absorbed dose in IPEC films, the mass absorption coefficients[29] for photons with an energy of 20 keV were used. The strong dependence of X-ray radiation coefficients on the atomic number of the absorber leads to silver ions having the greatest effect on the rate of absorbed dose of the sample (Table. 1), therefore, when using X-ray radiation, the rates of metal ion reduction and nanoparticle formation increase with their increasing content in IPEC films.[4,26,27] In this regard, comparative studies of the formation of nanoparticles in the samples were carried out for the same irradiation duration. It was determined earlier that in a sample with a 16 wt.% content the formation of silver nanoparticles is completed after an exposure duration of 60 min.[20] An irradiation duration of 15 min was chosen for the study of the starting stage of the formation of nanostructures.

Table 1. Dose rate of radiation (P) for components of the irradiated system

Sample	Silver ion content (wt.%)	P/Gy s^{-1}
Aqueous-alcoholic medium	—	16.23
IPEC film	0	10.71
	0.1	11.22
	2.0	21.09
	6.0	42.19
	16.0	94.44

Analysis of microphotographs shows that irradiation leads to the appearance of silver nanoparticles in films of PAA—PEI complexes with different silver ion content (Fig. 1). The microdiffraction patterns show clear ring reflections which correspond to interplanar distances: 2.35, 2.04, 1.45, and 1.23 Å (see Fig. 1, *b*), matching the crystal lattice of silver.[30] Thus, metal nanoparticles are formed as a result of radiation-induced reduction of silver ions in matrices of IPECs.

In the sample with an initial silver ion content of 0.1%, nanoparticles up to 20 nm in size are formed exclusively in the near-surface layer of the film when irradiated for 15 min (see Fig. 1, *a*), at this stage, the obtained nanoparticles have sizes up to 15 nm. Irradiation of the sample for 1 h leads not only to the formation of relatively large nanoparticles, having sizes up to 40 nm (see Fig. 1, *c*), in the near-surface layer, but also to the appearance of nanoparticles 1—5 nm in size within the film bulk (see Fig. 1, *d*). The density of nanoparticles in the near-surface layer increases with irradiation duration (see Fig. 1, *c*).

When the sample with an initial silver ion content of 2% is irradiated for 15 min, nanoparticles form not only on the surface, but also in the film bulk (Fig. 2, *a*—*c*). In this case, there are at least three distinct zones of nanoparticle formation (Fig. 2, *g*). Nanoparticles with sizes up to

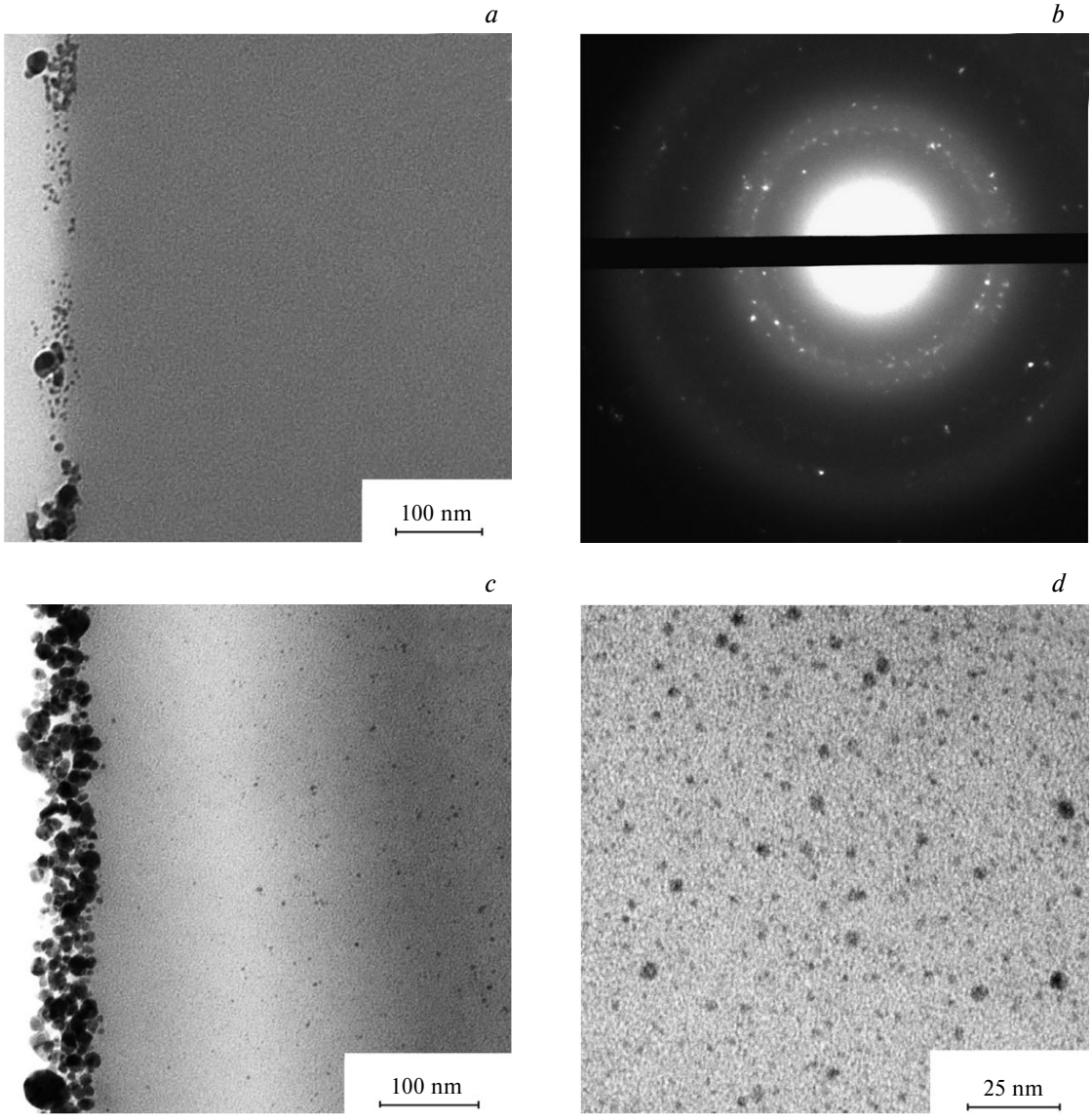

Fig. 1. Microphotographs of film cuts (sample irradiation duration: 15 (*a*), 60 (*c*), 60 min (*d*; depth 10 μm)) and microdiffraction pattern (*b*; sample irradiation duration 60 min) of complex PAA—PEI—Ag^+ with an initial silver ion content of 0.1 %.

30 nm are localized in the near-surface layer (zone I) (see Fig. 2, *a*). During the initial stage of formation, relatively small particles with sizes up to 5 nm predominate. Irradiation of this sample for 60 min leads to an increase in the nanoparticle size and the particle density of the surface layer (Fig. 2, *d*). In the layer located at a depth of 2—2.5 μm (zone II), the formation of relatively large particles, along with nanoparticles 1—5 nm in size, is observed (see Fig. 2, *b*, *e*, *g*). The sizes of these particles reach 8—20 nm when irradiated for 15 minutes (see Fig. 2, *b*), and an increase in the duration of exposure leads to the formation of nanoparticles up to 30 nm in size and the formation of nanoparticle aggregates (see Fig. 2, *e*). Finally, within the deeper layers of the film (zone III), nanoparticles having relatively small sizes (1—5 nm) are observed after irradiation durations of both 15 and 60 min (see Fig. 2, *c*, *f*, *g*).

Four zones of nanoparticle formation can be distinguished in the irradiated sample with a starting silver ion content of 6% (Fig. 3). Zones I, III, and IV (see Fig. 3, *g*) are practically the same as zones I, II, and III of the sample with an initial silver ion content of 2%. However, the thickness of the layer where relatively large nanoparticles form (zone III) increases considerably and becomes equal to about 5—8 μm (see Fig. 3, *a*, *d*, *g*). Microphotographs of film cuts also clearly show a layer about 150 nm thick (zone II; see Fig. 3, *a*, *d*), which is located immediately below the surface layer of the film. Nanoparticles up to 5 nm in size form in this zone both after short and long irradiation durations. No noticeable

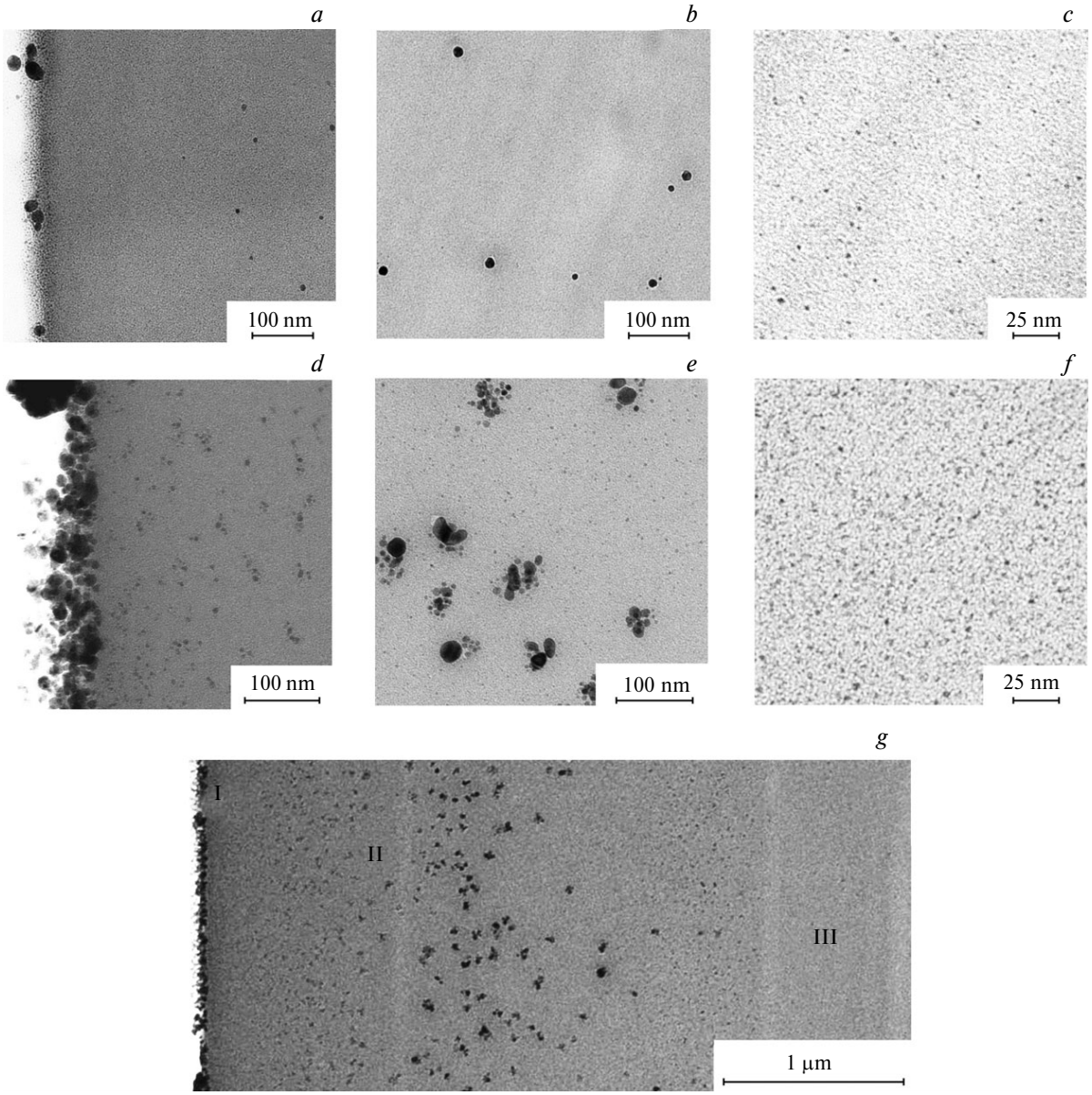

Fig. 2. Microphotographs of film cuts of complex PAA—PEI—Ag^+ with an initial silver ion content of 2%; sample irradiation duration 15 min (*a*), 15 min (*b*; depth 1.5 μm), 15 min (*c*; depth 6 μm), 60 min (*d*), 60 min (*e*; depth 1.5 μm), 60 min (*f*; depth 6 μm), and 60 min (*g*).

change in the size of nanoparticles is observed in this region with increasing irradiation duration.

Qualitatively similar processes are observed in the sample with an initial silver ion content of 16 wt.%. In this case, silver ion content is close to the maximum, which is 20 wt.% for PAA—PEI complexes.[19] The analysis of experimental results for this sample shows that the formation of nanoparticles takes place across four zones, as is the case for the sample with an initial silver ion content of 6%. The effect of the radiation dose on nanostructures in zones I and III, where relatively large nanoparticles form, for a sample with a silver ion content of 16% was studied previously.[20] A gradual increase of nanoparticle size with irradiation duration was observed. In this sample, the layer in which relatively large particles form reaches a depth of ~30 μm. Nanoparticle sizes remain relatively small in zone II and in the deeper layers of the film (zone IV) for the investigated irradiation interval (Fig. 4).

During radiation-initiated synthesis of nanoparticles in films immersed in aqueous-organic solutions, the external environment fraction makes up more than 90%. Due to this, a major role in the reduction of metal ions and the formation of nanoparticles is played by diffusion processes with the participation of products formed during the radiolysis of water.[4,19,20] Radiolysis of water can be schematically represented as follows:[11,24]

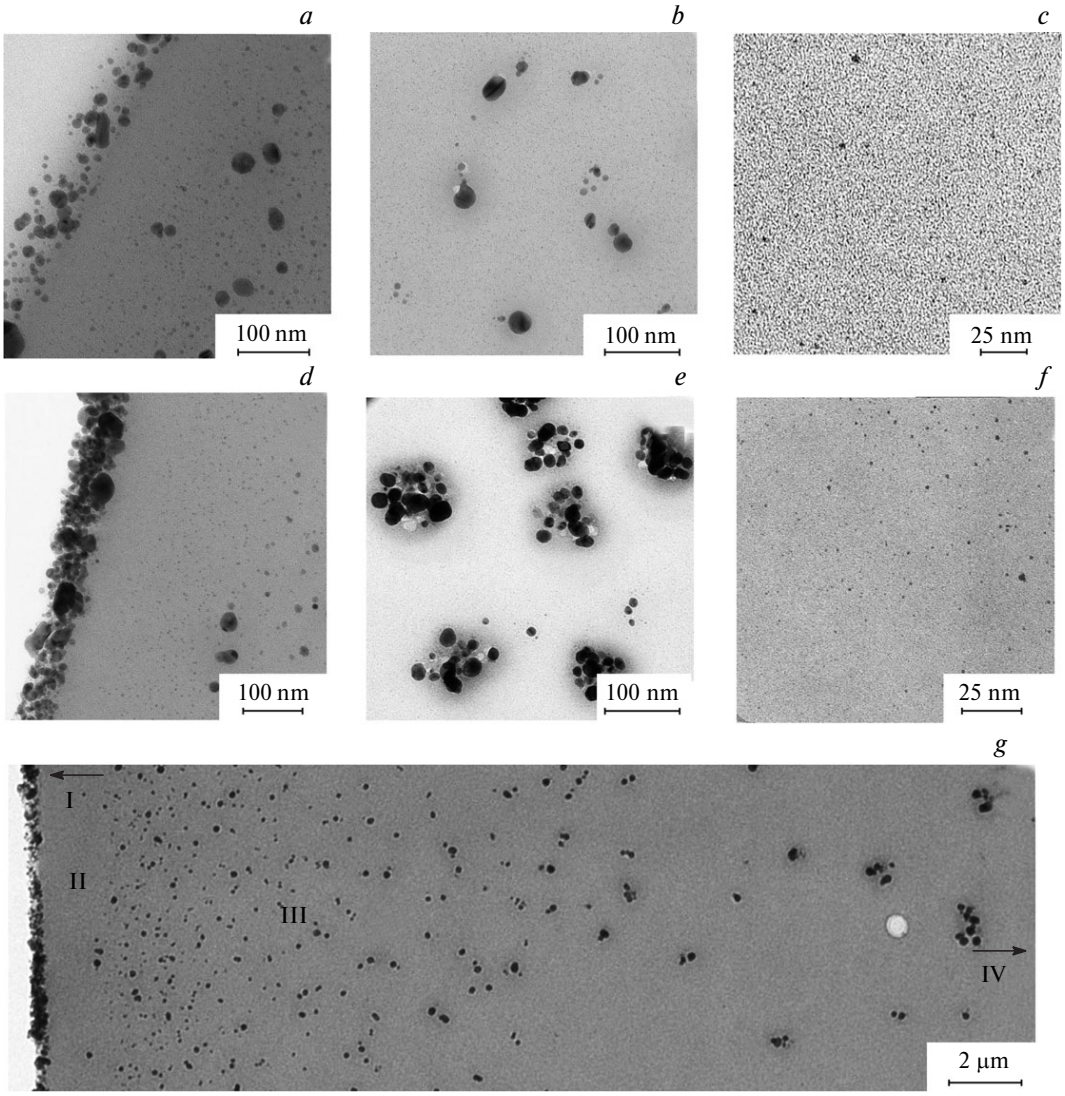

Fig. 3. Microphotographs of film cuts of complex PAA—PEI—Ag^+ with an initial silver ion content of 6%; sample irradiation duration 15 min (*a*), 15 min (*b*; depth 3 μm), 15 min (*c*; depth 20 μm), 60 min (*d*), 60 min (*e*; depth 3 μm), 60 min (*f*; depth 20 μm), 60 min (*g*).

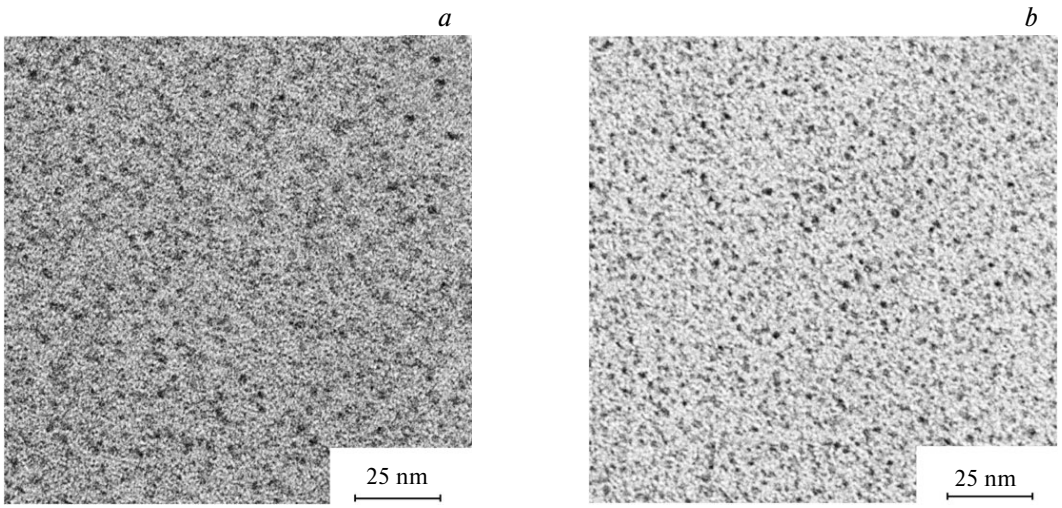

Fig. 4. Microphotographs of sample (zone IV) PAA—PEI—Ag^+ with an initial silver ion content of 16%; irradiation duration 15 min (*a*; depth 50 μm), 60 min (*b*; depth 50 μm).

$$H_2O \longrightarrow e^-_{aq},\ {}^{\bullet}OH,\ H_3O^+,\ H^{\bullet},\ H_2,\ H_2O_2,\ HO_2{}^{\bullet}. \qquad (1)$$

Exposure to ionizing radiation leads to the following being formed with the highest yield: hydrated electrons, which have an extremely high reduction potential (−2.9 V)[31], and ${}^{\bullet}OH$-radicals, which act as an oxidant. An amount of ethanol (10% ethanol content) was added to neutralize ${}^{\bullet}OH$-radicals and to create favorable conditions for the reduction of metal ions, resulting in the formation of the radical $Me{}^{\bullet}CHOH$ ($E^0_{Me{}^{\bullet}CHOH}$ = = −1.4 V)[11,31], which has reducing properties:

$$MeCH_2OH + {}^{\bullet}OH \longrightarrow Me{}^{\bullet}CHOH + H_2O. \qquad (2)$$

The oxidation of ethanol radicals leads to the formation of a weak reducing agent, namely acetaldehyde. Thus, only reducing particles are generated in aqueous-organic mixtures when using ethanol as an acceptor of ${}^{\bullet}OH$ radicals.

The mechanisms of radiation-chemical formation of silver nanoparticles have been studied in detail earlier.[24,32–35] In the first stage, silver ions are reduced to isolated atoms and clusters are formed:

$$(Ag)^+ + e^-_{aq} \longrightarrow (Ag)^0, \qquad (3)$$

$$(Ag)^0 + (Ag)^+ \longrightarrow (Ag_2)^+. \qquad (4)$$

As a result of reactions of silver atoms and ions, nanoparticles are obtained in successive processes of formation of clusters with a certain structure,[32,33,35] the so-called "magic" clusters:

$$(Ag_2)^+ \longrightarrow (Ag_3)^{2+} \longrightarrow (Ag_4)^{2+} \longrightarrow (Ag_8)^{2+}. \qquad (5)$$

The cluster $(Ag_8)^{2+}$ is quite stable, its lifetime reaches tens of minutes.[35] Growth of clusters results from the reduction of silver ions on their surface:

$$(Ag_m)^{n+} + (Ag)^+ \longrightarrow (Ag_{m+1})^{n+1} \longrightarrow (Ag_{m+1})^n, \qquad (6)$$

coalescence processes

$$(Ag_m)^{n+} + (Ag_k)^{g+} \longrightarrow (Ag_{m+k})^{(n+g)+} \qquad (7)$$

also lead to nanoparticle formation and growth.[11,24,32,33]

Since $E^0(Ag^+/Ag^0) = -1.8$ V,[31] a hydrated electron can carry out the reduction of silver ions to form isolated atoms (see reaction (3)). Thus, the nucleation process (see reactions (3)—(5)) is limited by reactions involving the strongest reducing agent. The reduction of silver ions on the surface of nanoparticles, which leads to nanoparticle growth (see reaction (6)), can occur due to reducing agents with lower reduction potentials, including acetaldehyde.[19,20]

The obtained results show similar regularities of nanoparticle formation near the surface of films in IPECs with different initial silver ion content (see Fig. 1—3). In the beginning, mainly relatively small nanoparticles form, and an increase of the radiation dose leads to an increase in the average nanoparticle size. In this region, the obtained nanoparticles are observed to have a relatively wide size distribution in the surface layer of films having a thickness of 50—80 nm for irradiation durations of both 15 and 60 min, which is due to the formation of nanoparticles in parallel processes of formation and growth.

The factor that has a decisive influence on nanoparticle formation is the use of X-ray radiation. In contrast to γ-radiation or accelerated electrons, the efficiency of the interaction of X-ray photons is critically dependent on the nature of the absorber. The rate of absorbed dose in the sample increases multiple times with an increase in metal ion concentration, because the mass absorption coefficients of metal ions and atoms are much higher (see Table 1) than those of elements that make up the polymer film and the aqueous-organic medium. This effect leads to an increase in the rate of formation of reducing radiolysis products and provides a growth in the rate of formation of metal nanoparticles in IPEC matrices with an increased metal ion content.[4,19,20,27] Diffusion of reducing radiolysis products from an aqueous-organic medium provides favorable conditions for the formation of nanoparticles on the surface of polymer films. When films of metal-polymer complexes are irradiated in an aqueous-organic medium, it is necessary to take into account the local distribution of the dose rate.[13] Ultrasmall metal nanoparticles formed in the initial stages[4,10,13,19,20,27] are strong absorbers of X-ray radiation, which leads to an increase the local dose rate near the film surface multiple times. As a result, the formation of metal nanostructures near the surface of polymer films self-accelerates.

The correlation between silver ion content and nanoparticle formation is mainly observed for the bulk of irradiated samples, which is related to the influence of silver ion concentration on the ratio of formation and growth processes of nanoparticles. In this case, nanoparticles up to 7 nm in size are formed in the film with an initial silver ion content of 0.1 wt.%, and their average sizes change little with increasing irradiation duration. The formation of relatively large nanoparticles is observed even for short durations of irradiation in films with a higher silver ion concentration. An increase in the radiation dose is accompanied by their growth. The analysis of microphotographs shows that the role of nanoparticle growth processes increases with silver ion content.

The necessity of taking into account the change in nanoparticle size occurring in parallel generation and growth processes in different zones of the polymer sample, the diffusion of reducing radiolysis products, and the transport of silver ions through the polymer matrix makes it practically impossible to quantitatively describe nanoparticle formation within the framework of formal kinetics. However, the analysis of the obtained results makes it possible to describe the specific features of nanostructure formation at a qualitative level.

Competition between nucleation and growth reactions is accompanied by the migration of silver ions through the polymer matrix due to the equalization of their concentration as ions are consumed in nanoparticle formation processes. The obtained results (see Fig. 1—3) demonstrate the formation of silver nanoparticles in zones regularly located throughout the film thickness, indicating the almost complete absence of nanoparticle migration within the polymer matrix. Under these conditions, the growth of nanoparticles occurs through the reduction of silver ions on the nanoparticle surface (see reaction (6)) practically without the contribution of coalescence processes (see reaction (7)). Thus, the probability of the formation of large nanoparticles will be determined by silver ion content in polymer films.

To interpret the results of the formation of relatively large nanoparticles in zones that are regularly located in the bulk of polymer films irradiated in an aqueous-organic medium (see Fig. 1—3), it should be kept in mind that according to EPR spectroscopic studies,[4,19,26] metal ions are evenly distributed within the matrix of PAA—PEI complexes in samples with different metal ion content. It is also necessary to take into account the scale of the radiation-initiated reactions of various reducing agents.[4,19,20,27] Hydrated electrons, which facilitate nucleation processes, can migrate over distances of the order of hundreds of nanometers. In the case of samples with a thickness of 150 μm, these processes proceed due to reactions of electrons formed within the swollen film or near its boundaries. Both types of active particles (hydrated electrons and alcohol radicals), as well as acetaldehyde, can enable the growth of metal clusters and nanoparticles.[4,19,20,27] The lifetime of hydrated electrons is several microseconds, however, high reaction rates[36] of these active particles ensure the high efficiency of their participation in the reduction of metal ions. Alcohol radicals, like hydrated electrons, ensure the formation of nanoparticles in local processes with high yields.[37] Unlike radical species, acetaldehyde is a relatively stable product of radiolysis. The aqueous-alcoholic medium makes up most of the irradiated sample, therefore, acetaldehyde is mainly formed within it. Due to diffusion processes, the participation of "long-range" reactions of the relatively stable acetaldehyde from the environment plays a major role in the growth of silver nanoparticles in films.[4,19,20,27] It is logical to assume that nanoparticle growth is determined by the diffusion of acetaldehyde from the solution and the transport of silver ions from the deeper layers of the film (Fig. 5).

The forefront of nanoparticle formation, located near the film surface, is characterized by relatively high acetaldehyde concentrations. As acetaldehyde becomes depleted, silver ion concentration begins to exert an increasing influence on the rate of nanoparticle formation. According to this interpretation, the depth of the layer where nanoparticles form will increase with silver ion content in the film. Indeed, analysis of the experimental results demonstrates an increase in the depth of the layer of formation of metal nanostructures with increasing metal ion content. The presence of a zone with relatively small nanoparticles in the film bulk can be explained by a deficiency of acetaldehyde due to its gradual consumption in reduction reactions.

Microphotographs of irradiated samples with an initial silver ion content of 6 and 16 wt.% show regions 150—250 nm wide (see Figs 3 and 4) located immediately behind the surface zone of nanoparticle formation. Only nanoparticles up to 5 nm in size are localized in this zone, regardless of irradiation duration. During nanoparticle formation, silver ions migrate from the film bulk to the ligand vacancies which appeared near the sample surface. This leads to the formation of a near-surface zone (zone II, see Fig. 3, *g*), which is free of relatively large nanoparticles. Such a drainage zone for silver ions is weakly expressed in the sample containing 2% silver ions, compared to samples with a higher starting metal ion content.

The observed effect can be explained by the fact that the efficiency of X-ray absorption increases with silver ion content in the samples, which leads to an increase of the radiation dose absorbed by the samples, and, consequently, to an increase of the rate of formation of reducing products near the film surface. Thus, an increase in the rate of nanoparticle formation will lead to an increase in the ef-

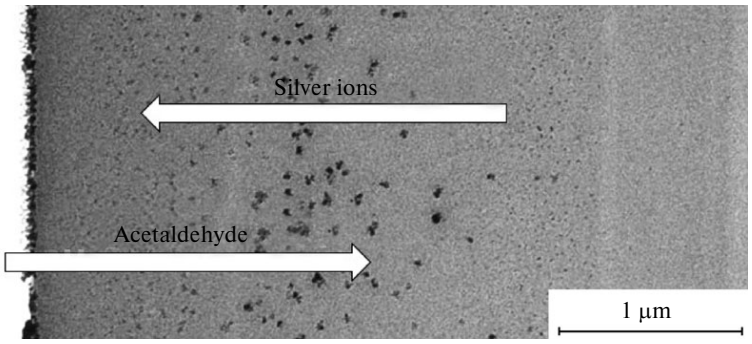

Fig. 5. Diagram of the formation of silver nanoparticles in the complex PAA—PEI.

ficiency of the transport of silver ions to the formed ligand vacancies and to the surface of the forming nanoparticles. Consequently, the observed effect, caused by the drainage of silver ions, should be most pronounced in samples with a relatively high silver ion content.

The formation of nanoparticle aggregates (see Fig. 2, *e*, Fig. 3, *e*) is another specific feature of X-ray irradiation. This process was investigated in detail earlier[20] for a sample containing 16 wt.% silver ions. The obtained silver nanoparticles are strong absorbers of X-ray radiation, which leads to an increase in the rate of formation of reducing radiolysis products near the resulting nanoparticles. X-ray irradiation leads to the formation of new small "daughter" nanoparticles and clusters at distances up to 70 nm from the primary particles. Their origin is related to the local component of the photoelectron spectrum resulting from the ionization of K-shells of silver atoms. During the next stages, an increasing dose leads to the growth of both primary and daughter nanoparticles due to the reduction of silver ions on their surface. As a result, metal nanostructures having the appearance of nanoparticle aggregates are formed.

The obtained results show that a special feature of the use of X-ray radiation is not only a high efficiency of nanostructure formation in polymer systems with a high metal ion content, but also a specific spatial organization of silver nanoparticles. The local transfer of energy absorbed by silver nanoparticles leads to the formation of secondary metal nanostructures that appear as aggregates of nanoparticles. However, the most important aspect from a practical point of view is the predominant localization of metal nanostructures near the surface of polymer films. This occurs due to specifics of interaction of X-ray radiation with metal-polymer complexes under conditions of diffusion of reducing radiolysis products from the aqueous-organic medium. The localization of nanoparticles on the surface of the matrix makes the metal nanostructures accessible for reagents or compounds being detected, which is a promising feature for the development of biosensors, catalysts, water purification systems, as well as antibacterial materials. These studies reveal the effect of silver ion content on the specific features of nanoparticle formation in IPECs, which makes possible the controlled formation of various types of nanostructures in polymer films and coatings. Electron microscopy revealed that the formation of metal nanoparticles occurs in zones regularly located in the film bulk. Structures formed within the bulk of samples with a low silver ion content (0.1%) have the highest mass ratio of metal nanoparticles on the surface of films in comparison to their bulk. This is a result of the transport of silver ions through the polymer matrix to the surface and the low probability of nanoparticle growth within the film bulk. In this case, relatively small nanoparticles (1—5 nm) form within the film bulk, which is important for the development of methods of obtaining materials with catalytic or electrocatalytic activity. The efficiency of the formation of relatively large nanoparticles with a wider silver-containing layer in the film bulk increases with the initial silver ion content in IPECs. These nanocomposites can be applied in the development of bactericidal film materials used under conditions of gradual removal of the outer layers.

This work was financially supported by the Russian Foundation for Basic Research (Project No. 18-03-00608).

References

1. J. Dai, M. L. Bruening, *Nano Lett.*, 2002, **2**, 497; DOI: 10.1021/nl025547l.
2. M. L. Bruening, D. M. Dotzauer, P. Jain, L. G. Ouyang, L. Baker, *Langmuir*, 2008, **24**, 7663; DOI: 10.1021/la800179z.
3. D. M. Dotzauer, A. Abusaloua, S. Miachon, J.-A. Dalmon, M. L. Bruening, *Appl. Catal. B Environ.*, 2009, **91**, 180; DOI: 10.1016/j.apcatb.2009.05.022.
4. A. A. Zezin, D. I. Klimov, E. A. Zezina, K. V. Mkrtchyan, V. I. Feldman, *Radiat. Phys. Chem.*, 2020, **169**, 108076; DOI: 10.1016/j.radphyschem.2018.11.030.
5. D. V. Pergushov, A. A. Zezin, A. B. Zezin, A. H. E. Müller, *Adv. Polym. Sci.*, 2014, **255**, 173; DOI: 10.1007/12_2012_182.
6. N. L. Rosi, C. A. Mirkin, *Chem. Rev.*, 2005, **105**, 1547; DOI: 10.1021/cr030067f.
7. S. Fathalipour, S. Ahunbar, *Polym. Sci., Ser. B*, 2019, **61**, 663; DOI: 10.1134/s1560090419050038.
8. N. A. Samoilova, M. A. Krayukhina, O. V. Vyshivannaya, I. V. Blagodatskikh, D. A. Popov, N. M. Anuchina, I. A. Yamskov, *Russ. Chem. Bull.*, 2018, **67**, 1010; DOI: 10.1007/s11172-018-2172-x.
9. D. I. Klimov, E. A. Zezina, V. C. Lipik, S. S. Abramchuk, A. A. Yaroslavov, V. I. Feldman, A. A. Zezin, *Radiat. Phys. Chem.*, 2019, **162**, 23; DOI: 10.1016/j.radphyschem.2019.04.027.
10. A. A. Zezin, *Polym. Sci., Ser. C*, 2016, **58**, 118; DOI: 10.1134/S1811238216010136.
11. J. Belloni, *Catal. Today*, 2006, **113**, 141; DOI: 10.1016/j.cattod.2005.11.082.
12. V. A. Aleksandrova, L. N. Shirokova, *Polym. Sci., Ser. B*, 2018, **60**, 727; DOI: 10.1134/s1560090418060027.
13. A. A. Zezin, *Polym. Sci., Ser. A*, 2019, **61**, 754; DOI: 10.1134/S0965545X19060154.
14. F. Schacher, E. Betthausen, A. Walther, H. Schmalz, D. V. Pergushov, A. H. E. Müller, *ACS Nano*, 2009, **3**, 2095; DOI: 10.1021/nn900110s.
15. F. H. Schacher, T. Rudolph, M. Drechsler, A. H. E. Müller, *Nanoscale*, 2011, **3**, 288; DOI: 10.1039/c0nr00649a.
16. Z. Lei, X. Wei, L. Zhang, S. Bi, *Colloids Surf. A: Physicochem. Eng. Asp.*, 2008, **317**, 705; DOI: 10.1016/j.colsurfa.2007.12.006.
17. V. Demchenko, S. Riabov, V. Shtompel′, *Nanoscale Res. Lett.*, 2017, **12**, 235; DOI: 10.1186/s11671-017-1967-2.
18. V. Demchenko, V. Shtompel′, S. Riabov, *Eur. Polym. J.*, 2016, **75**, 310; DOI: 10.1016/j.eurpolymj.2016.01.004.
19. A. A. Zezin, V. I. Feldman, S. S. Abramchuk, V. K. Ivanchenko, E. A. Zezina, N. A. Shmakova, V. I. Schvedunov, *Polym. Sci., Ser. C*, 2011. **53**, 61; DOI: 10.1134/S1811238211060038.
20. V. I. Feldman, A. A. Zezin, S. S. Abramchuk, E. A. Zezina, *J. Phys. Chem. C*, 2013, **117**, 7286; DOI: 10.1021/jp3090765.

21. A. G. Chmielewski, D. K. Chmielewska, J. Michalik, M. H. Sampa, *Nucl. Instrum. Methods Phys. Res. B*, 2007, **265**, 339; DOI: 10.1016/j.nimb.2007.08.069.
22. W. Abidi, H. Remita, *Recent Pat. Eng.*, 2010, **4**, 170; DOI: 10.2174/187221210794578556.
23. R. Yoksan, S. Chirachanchai, *Mater. Chem. Phys.*, 2009, **115**, 296; DOI: 10. 1016/j.matchemphys.2008.12.001.
24. B. G. Ershov, E. V. Abkhalimov, *Colloid J.*, 2006, **68**, 417; DOI: 10.1134/s1061933x06040041.
25. D. I. Klimov, E. A. Zezina, S. B. Zezin, M. Yang, F. Wang, V. I. Shvedunov, A. A. Zezin, *Radiat. Phys. Chem.*, 2018, **142**, 65; DOI: 10.1016/j.radphyschem.2017.02.034.
26. A. A. Zezin, V. I. Feldman, A. V. Dudnikov, S. B. Zezin, S. S. Abramchuk, S. I. Belopushkin, *High Energy Chem.*, 2009, **43**, 100; DOI: 10.1134/S0018143909020064.
27. A. A. Zezin, V. I. Feldman, E. A. Zezina, S. I. Belopushkin, E. V. Tsybina, S. S. Abramchuk, S. B. Zezin, *High Energy Chem.*, 2011, **45**, 99; DOI: 10.1134/S0018143911020147.
28. A. S. Pozdnyakov, G. F. Prozorova, S. S. Abramchuk, V. I. Feldman, A. A. Zezin, E. A. Zezina, A. I. Emel′yanov, *Radiat. Phys. Chem.*, 2019, **158**, 115; DOI: 10.1016/j.radphyschem. 2019.01.019.
29. J. H. Hubbel, S. M. Seltzer, *Radiat. Phys. Division*, PML, NIST, 1995; DOI: https://dx.doi.org/10.18434/T4D01F.
30. J. D. Hanawalt, H. W. Rinn, L. K. Frevel, *Industr. Eng. Chem. Anal. Ed.*, 1938, **10**, 457; DOI: 10.1021/ac50125a001.
31. P. Wardman, *J. Phys. Chem. Ref. Data*, 1989, **18**, 1637; DOI: 10.1063/1.555843.
32. B. G. Ershov, E. Janata, A. Henglein, *J. Phys. Chem.*, 1993, **97**, 339; DOI: 10.1021/j100104a013.
33. M. Mostafavi, N. Keghouche, M.-O. Delcourt, J. Belloni, *Chem. Phys. Lett.*, 1990, **167**, 193; DOI: 10.1016/0009-2614(90)85004-v.
34. M. Mostafavi, N. Keghouche, M.-O. Delcourt, *Chem. Phys. Lett.*, 1990, **169**, 81; DOI: 10.1016/0009-2614(90)85169-d.
35. B. G. Ershov, *J. Phys. Chem.*, 1998, **102**, 10663; DOI: 10.1021/jp981906i.
36. M. Anbar, M. Bambenek, A. B. Ross, *Selected Specific Rates of Reactions of Transients from Water in Aqueous Solution, I. Hydrated Electron*, NSRDS-NBS 43, National Bureau of Standards, U.S. Department of Commerce, Washington, 1973; DOI: 10.2172/4445489.
37. B. G. Ershov, *Russ. Chem. Bull.*, 1994, **43**, 16; DOI: 10.1007/bf00699128.

Received November 30, 2019;
in revised form April 8, 2020;
accepted May 31, 2020